EXPERIMENTAL AND NUMERICAL ANALYSIS OF A PHASE CHANGE STORAGE UNIT

Maike Johnson
Nils Breidenbach
Doerte Laing
German Aerospace Center (DLR)
Pfaffenwaldring 38-40
70597 Stuttgart, Germany
maike.johnson@dlr.de

Dr. Bernd Hachmann
F.W. Broekelmann Aluminiumwerk GmbH & Co. KG
Oesterweg 14
59469 Ense-Hoeingen, Germany

ABSTRACT

Thermal storage technologies are key components for increasing energy efficiency and assisting the integration of regenerative energy sources in the energy market. One type of thermal energy storage is latent heat storage, which makes use of the large amount of enthalpy that can be stored during the phase change of a storage material, and is an interesting storage technology for both high temperature and process steam processes. However, the rate of heat transfer into and out of the storage is a limiting factor for fast discharges, due to the inherently low rate of heat transfer of the storage materials. In order to enhance the rate of heat transfer in latent heat storage units, heat transfer structures have been developed and tested at DLR. Various fin designs have been analyzed and tested. To analyze the effectiveness of more complex geometries, a finite element method analysis method has been developed. Concurrently, physical storage units have been tested. Based on the results from the testing of a fin design in a demonstration storage unit, a new fin was designed. This fin shows good results in the laboratory environment. In this paper, the results from the finite element method analysis and those of a lab-scale latent heat storage unit with the new fin design are compared and discussed.

1. INTRODUCTION

Storage in general buffers a component, in this case thermal energy, for use at a later time. The buffer can be used to make one system usable for a longer period of time, as in solar thermal power plants, or to connect two systems that supply and demand thermal energy at different times as is more common in process heat applications.

Thermal energy storages are typically classified by their storage medium. These are sensible, latent, and thermo-chemical. In sensible storage, the storage remains in one phase and changes temperature as the enthalpy level in the medium changes. A commercially available example of sensible storage is two-tank molten salt storage. By comparison, in latent energy storage the storage material is a phase change material (PCM) that changes phase from, for example, solid to liquid as more energy is charged into the storage. This makes use of the large amount of enthalpy that can be stored during the phase change of a storage material, and results in a higher storage capacity per unit volume than typically found in sensible storage materials. This paper describes research on latent energy storage units. In the third category, thermo-chemical storage, the storage material undergoes a chemical reaction that stores or releases thermal energy. However, these types of storage systems are still in the basic research stage.

Due to their relative compactness, latent heat storages are an interesting storage technology for both high temperature and industrial steam processes. Since a storage unit is a combining link in the chain between supply and demand of heat, it has to be adapted for each particular application. This includes the temperatures (selection of the phase change material), capacity (PCM volume), flow (tube diameter/number of tubes) and the power level. The power level is a function of the overall heat transfer coefficient.

2. DESCRIPTION OF PCM STORAGES

In design concepts that have thus far been proven for high temperature latent heat storage, a tube bundle is immersed in the storage medium/PCM and acts as a heat exchanger between the storage medium and the heat transfer medium (HTM). The HTM flows through the tubing, transferring heat to and from the tubing. The tubing transfers the heat to and from the PCM by conduction. In the PCM, heat is transferred via conduction and, in the liquid state, also by

natural convection. The overall heat transfer resistance is a summation of all of the system components. This includes the heat transfer h through forced convection of the HTM flowing through the tubing and the thermal conductivities k1, k2 of the tubing and the storage material.

The thermal conductivity k of PCMs is inherent to the storage material and is typically low and a limiting factor (Table 3). In the solid state, the PCM acts almost as an insulator. During the discharge of stored heat the storage material solidifies from the heat transfer surface outwards, and is thus a barrier between the heat transfer medium HTM and the still liquid storage material (Fig. 1).

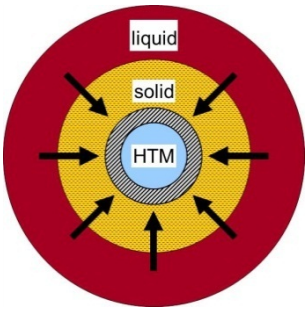

Fig. 1: Schematic of heat transfer from liquid through solid PCM and the steel tube to the HTM.

Although the thermal conductivity in liquid PCM is not higher, natural convection occurs between the particles of varying density, so that all in all a higher heat transfer rate occurs. Therefore, to increase the power level possible in latent heat storage systems, heat transfer structures have been developed that increase the indirect contact surface area A between the PCM and the heat transfer medium. These heat transfer structures are made of materials with a high thermal conductivity k, such as graphite (1). These structures reduce the thickness of the boundary barrier layer that forms between the heat transfer medium and the not-yet-discharged storage material. These heat transfer structures also increase the total heat transfer coefficient during charging. However, the boundary barrier is less of a problem during charging. Therefore, thermal discharge rates are typically discussed. Since the simulation model used does not include natural convection, charging cycles are discussed and analyzed in this paper.

In order to increase the possible power level, the surface area of the tubing has been increased with exterior fins. Both sheet, radial, and axial fins have been used in various storage test units and have proven the design concept ((1), (2), (3)). Other concepts for increasing the overall heat transfer coefficient have also been reported (1).

In a latent heat storage system, the storage medium changes phase. This phase change is typically solid↔liquid, though theoretically the changes from solid↔solid and liquid↔gaseous are also possible (4). During the phase transitions, the storage medium undergoes an isothermal stage, during which the latent energy is stored or is released from the system (Fig. 2). If the heat transfer medium is a single phase fluid, the temperature gradients between the storage medium and the heat transfer medium vary throughout the charging or discharging process (Fig. 2). The slope of the sensible heat change depends on the heat capacity of the HTM, so that the curves in Fig. 2 are only an example. This results in a less efficient heat transfer. If the heat transfer medium changes phase simultaneously with the storage medium, the temperature gradient can be nearly constant throughout operation (Fig. 2). For this reason, latent heat storage is quite suitable for water↔steam systems on the HTM side of the storage. These are common, for example, in power plant cycles.

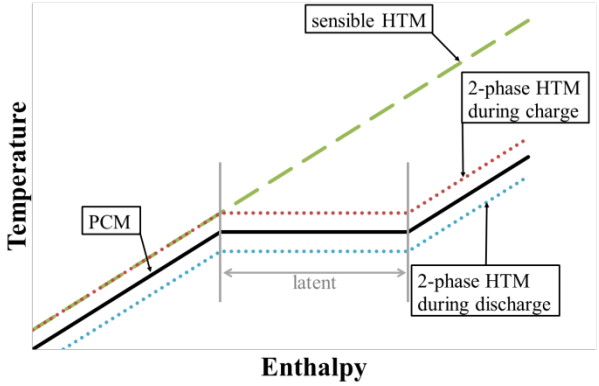

Fig. 2: Temperature-Enthalpy diagram for latent heat storage showing both a 1-phase and 2-phase heat transfer medium (adapted from (1) and (4)). Solid line, PCM; dashed lines, sensible HTM in charging and discharging; dotted lines, 2-phase HTM in charging and discharging

For heat exchange to occur in the storage unit, there needs to be a temperature gradient, both for charging and discharging. This means that the HTM temperature for discharging heat needs to be lower and for charging higher than the phase change temperature of the storage material (Fig. 2, red dotted line for charging and blue for discharging). In a water/steam process, this results in higher pressures in the charging system and lower pressures in the discharging systems. These differences must be considered in the system design.

In the sheet fin design, each single fin, graphite in the case of (1), is a thin sheet with holes stamped into it for the heat transfer tubes. These sheets are placed over the tube ends and moved axially down the tube into position,

forming a connected fin across all of the tubes. This bundle with headers is then surrounded by PCM in a container. The holes for the tubes are stamped into the sheets. Although this fin design was proven in (1), the temperature limitations and high costs for graphite make this a less attractive fin concept. The fin design requires very tight production tolerances to ensure that the stamped holes for tubing result in good contact with all of the tubes. Due to density differences between liquid and solid PCM, the design is only practicable for horizontal storage unit design. Evaporator storages, which are more interesting for latent heat storages, as discussed previously, optimally have a vertical build, so that the density differences in the water/steam HTM side also are optimally considered in the design process.

A radial fin design was proven to be effective in a demonstration storage unit (2). This unit was a condenser/evaporator and the heat transfer medium was water/steam. The fin used in this design was a radial disk fin, with a one centimeter distance between fins. These fins are mounted by sliding each fin over the end of and down the tube into position. The disks are equipped with holes to allow the melting salt to naturally circulate and expand in the storage unit, so that even though the disks have a horizontal surface, they can be assembled in a vertical evaporator build. The results from this storage are well documented (2).

In a further development of the fin design, aimed at simplifying the assembly of larger storage units and at reducing production costs, axial fins were designed, analyzed and tested in cooperation with F.W. Broekelmann Aluminiumwerk GmbH & Co. KG. These fins are made of extruded aluminum alloy. Inherent to the extrusion process, the fin structure is constant along the length of the tubing. This fin concept is therefore optimal for vertically oriented storage units, as the melt front in the PCM also extends radially from the tubing and the molten PCM (with a lower density) can freely expand along the tube axis. In extrusion processes, the costs for tooling are high. Therefore, it is critical to analyze a design for both production feasibility and effectiveness prior to tooling.

An axial fin design of the axial fin concept was assembled and tested in a lab-scale storage module and was concurrently analyzed with the finite element method (FEM) software ANSYS ®. Our experimental testing and simulations are presented in this paper.

3. EXPERIMENTAL TESTING

The experimental testing as reported in (2) was conducted on a lab-scale storage module integrated in a thermal oil heating and cooling loop. The storage module was equipped with thermocouples and the test rig was equipped with resistance thermometers and meters for pressure and flow. The goal of this testing was to evaluate the axial fin design as well as to validate the models and FEM simulations.

3.1. Fin and storage unit design

The axial fin we developed for latent heat storage is an extruded element. Two elements were clipped (5) to a tube to affix the fin halves. The clips were made of spring steel. A hexagonal design was selected since it results in an optimal use of the area between tubes in a triangular tube alignment. Due to limitations in extrusion feasibility, the ‘branches’ of the fins were only semi-regularly spaced around the entire fin area. Prior simulations showed a good temperature distribution throughout the PCM surrounding the heat transfer structure fins in this design. The fin design tested, as mounted in the storage module, is shown in Fig. 3.

Finned tubes are oriented along various axes relative to one another (Fig. 3). This is to prohibit fin sides with fewer branches abutting to similarly sparsely branched sides.

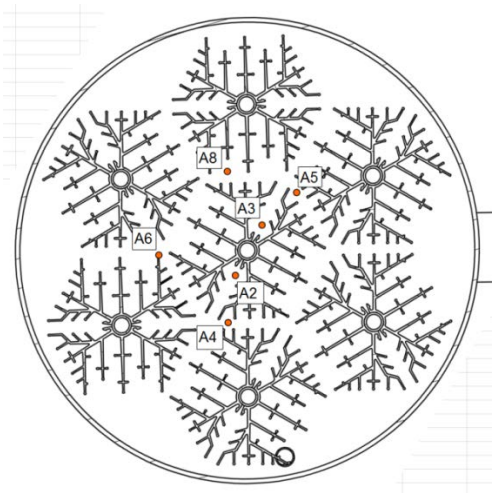

Fig. 3: Finned tube and thermocouple arrangement in a storage module, shown on the ‘A’ measurement level; red dots denote thermocouple placements, labeled A2-A8.

The design parameters as shown in Table 1 as well as the tube arrangement in Fig. 3 allowed for the testing of a single, central finned tube that is isolated from exterior losses by the surrounding six finned tubes. Also shown in Fig. 3 are the positions of the thermocouples on one level of the storage unit. These thermocouples are placed at the same level at about mid-height of the vertical storage unit to ascertain the temperature distribution about this centrally located finned tube. Other thermocouple layers were placed throughout the storage module. Since layer A was the furthest from external losses, it is analyzed here.

TABLE 1: STORAGE UNIT DESIGN PARAMETERS

Fin type	axial, aluminum
Tube length	1 m
No. of tubes	7
Storage medium weight	ca. 320 kg
Storage unit dimensions, w/o insulation	0.5 m ø x 1.8 m
Storage capacity	ca. 15 kWh

3.2. Test Loop & Test Program

The storage module was integrated for the test program in a thermal oil heating/cooling test rig loop. The heat transfer medium in the rig is Syltherm 800 oil; the rig is pressurized so that the thermal oil remains liquid during operation. The test rig was a simple heating/cooling loop with an electric heater as the heat source, an air cooler as the heat sink, a pump and measurement sensors for flow, temperature and pressure.

2.3 Experimental results

Various experiments were run on this test rig, documenting both discharging and charging cycles and with varied volumetric flow rates and temperature gradients. Shown in Fig. 4 and Fig. 5 are the results of charging and discharging, respectively, at 3.9 m³/h between 280 °C and 330 °C. These temperature results were as expected. Thermocouple A6, which is attached to a fin but furthest from a HTM tube (see Fig. 3), has the shortest plateau at the phase change temperature. Thermocouples A2 and A3, symmetrically placed near the inner tube, had the next shortest phase-change plateau. Thermocouple A8, furthest from any heat transfer structure, took the longest to complete the charging or discharging cycle.

Inset in Fig. 4 is a detail of the end of the phase change shown by the steep change in temperature. This detail shows that thermocouples A2, A3, A4 and A8 had a very steep incline after phase change was completed. This then flattened shortly thereafter. Thus far it has been assumed that the PCM that is already melted at the melt front is somewhat superheated. Particles around the thermocouple are fixed until phase change has been completed. These particles, due to the higher temperatures of the already melted particles at the melt front then naturally circulate, causing an initial rise in temperature. This rise then flattens as the melt front moves further away from the thermocouple. This phenomenon needs to be further analyzed.

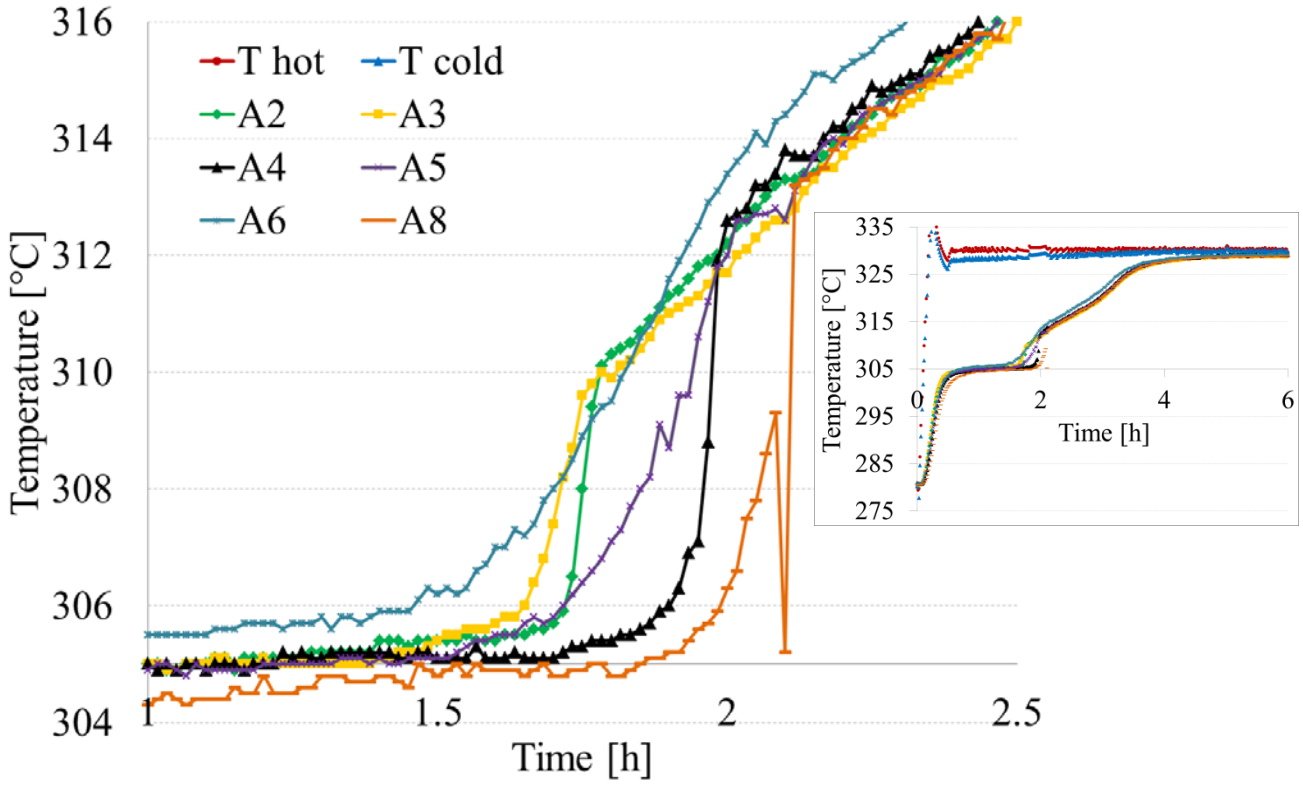

Fig. 4: Detail of charging at 3.9 m³/h from 280 °C to 330 °C; complete charge overview to the right.

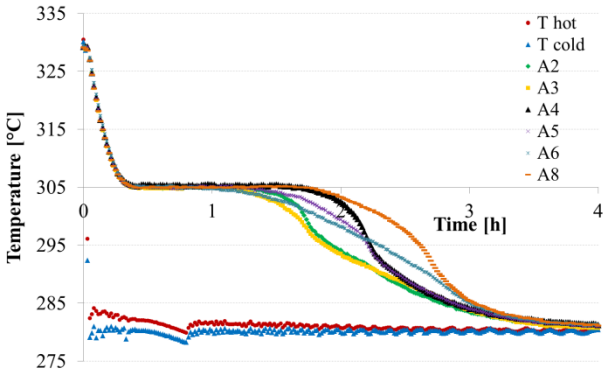

Fig. 5: Discharging at 3.9 m³/h from 330 °C to 280 °C.

In balancing the energy in an experimental unit, various factors were analyzed, e.g. inlet and outlet temperatures. Due to losses to the environment, which, when compared with the volume of the storage unit measured, were large, this comparison only offered a limited balancing of energies. We also compared thermocouple temperatures in one level with the HTM temperature. However, a determination of the experimental temperature within the tubes was not possible. The gradient between inlet and outlet temperatures was due not only to heat transfer from the HTM to the storage material along the entire tube length but also to the aforementioned losses to environment, so that a determination of the temperature of the HTM at both a time and location within the storage for balancing or comparison reasons was not possible. The energy balance is discussed in greater detail in (3).

For the tests on the storage unit, the storage unit was charged to an initial temperature until it could be assumed to be steady-state. Then a temperature was applied to the HTM as a step function and the unit was charged long enough so that steady-state conditions were again achieved. The unit was considered charged or discharged once this state was achieved. However, the storage material finished changing phase before the end temperature was achieved. In analyzing the slopes of the charging and discharging cycles, it was difficult to define either the charging or the completion of the phase change. Due to the sharp change in slope from almost zero slope to very positive, it is visible when the individual thermocouples measurement areas have completed phase change, but not the entire volume is captured with these thermocouples. On the other hand, the analysis only of the time at which all of the thermocouples have reached a steady-state condition would not give enough information for planning future designs, as the power level is higher during the phase change than in the time thereafter (2). The design of the storage module was to prove the extruded fin design. These results were then used to being validation of simulation models developed concurrently. Analysis of the data shows that instrumentation in future modules will need to be adapted in order to fully validate a simulation model.

4. SIMULATION OF HEAT TRANSFER STRUCTURES

Latent heat storage can, to a certain extent, be calculated analytically (6). However, with the inclusion of heat transfer structures and complicated geometries, calculations of the phase change front or charge status are only possible via modeling and simulations. The heat transfer structure analysis discussed here has a complex geometry, resulting in a complex simulation. ANSYS ® 14.0 MechanicalTM was used to simulate the design with a finite element analysis. One half of the fin design as it was modeled is shown in Fig. 6. Although symmetry exists to further halve this design, this leads to poor meshing in the central ‘branch’ of the heat transfer structure. As the fin is not actually symmetrical over the three sides when assembled into a multi-tube assembly, simulations were also conducted with all seven tubes as shown in Fig. 3. As this simulation was a much larger model needing much more computation time, models of a half fin were conducted with various parameters. The seven-faced simulation is discussed below.

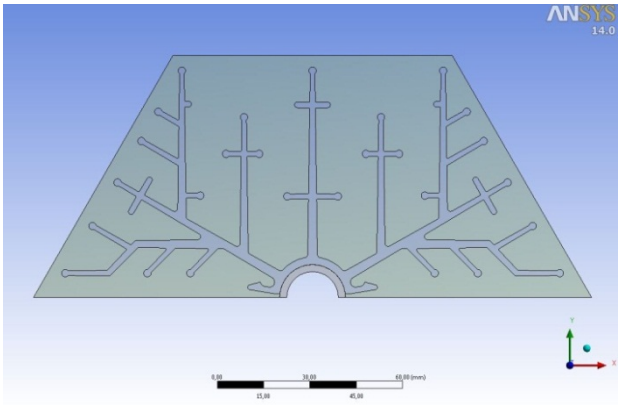

Fig. 6: Geometry model shown with the aluminum fin model in grey, steel tube in pink and surrounding PCM in green.

4.1. Description of simulation

A two-dimensional model in ANSYS ® 14.0 MechanicalTM was set up with transient thermal parameters. The goal of the simulations was to influence the layout and design of the fins before they were tooled, so that the temperature distribution and melt front growth would be evenly balanced in a finned tube or in a finned tube group. This goal allowed for a comparative simulation, so that exact times or values would not be not as critical as would be an analysis of the distribution paired with the production capabilities in determining further layout design. On the other hand, with a

quantitatively validated model, design predictions for future storages regarding the charge and discharge power in a storage could be made. This would call for a better model for future designs.

In these simulations, the model was applied with an initial temperature and then a forced convection at a specified temperature was applied to the internal wall of the steel tube. As the model is a two-dimensional slice of a three-dimensional storage unit, simplification was necessary. In a three-dimensional storage unit, especially with a sensible heat transfer medium, there are temperature gradients from one end of the heat transfer tube to the other. This was not taken into account in these simulations.

In order to simulate the phase change of the PCM, the enthalpy was coded in the ANSYS ® APDL language for the model parts requiring PCM. The material data used are shown in Table 2 and Table 3.

TABLE 2: MATERIAL PROPERTIES FOR STEEL AND ALUMINUM

Property/Material	Steel 1.4571	Aluminum 6060
Thermal conductivity, solid [W/(m·K)]	16.3	210
Density, solid [kg/m³]	7980	2700
Specific heat [J/(kg·K)]	490	1020 (300°C), 1110 (500°C)

TABLE 3: MATERIAL PROPERTIES FOR PCM (7)

Property/Material	Sodium nitrate ($NaNO_3$)
Thermal conductivity *k*, solid/ liquid [W/(m·K)]	0.6/ 0.514
Density, solid [kg/m³]	2260 (25°C), 2113 (305°C)
Density, liquid [kg/m³]	1908
Specific heat [J/(kg·K)]	1655
Melting temperature [°C]	305
Latent heat [J/kg]	178,000

The enthalpy definition in ANSYS ® is a semi-step function, where the enthalpy increase is over a one degree span from, in this case, 305 °C to 306 °C. This step is shown in Fig. 7.

For the transient thermal simulations, auto time stepping was set to 'on' with the initial time step adjusted to the element edge length; time integration and a direct solver

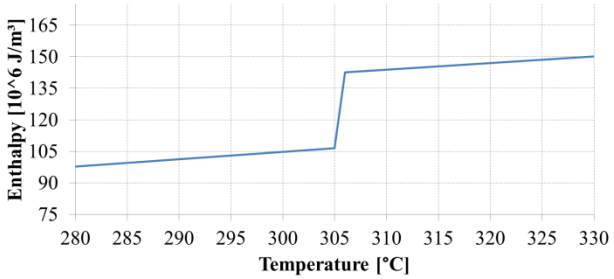

Fig. 7: Enthalpy step for PCM Material

were used. The initial temperature of the model was set to a uniform Tinitial=280 °C and the inner side of the steel tube was given a convective load with a temperature Tstep=330 °C to allow for comparison with experimental results. This heat transfer coefficient h was estimated based on the experimental parameters. Due to the various formulas for estimating the Nusselt number, an average value of h=750 W/(m²·K) was used.

The geometry was meshed with the ANSYS ® mesher. Mapped face meshing was set on the steel tube, and a uniform quad/tri method on both the PCM and the fin. The simulation was set to increase relevance on proximity and curvature, so that the areas of heat transfer had a better mesh than the outer PCM areas. A mesh study was conducted. The results from 3 meshes were compared (Table 4). The medium mesh was used for further calculations.

TABLE 4: MESH ANALYSIS PARAMETERS

Mesh	Elements	Elapsed time [s]	Melt time Probe 5 [s]
Rough	3384	360	12120
Medium	37955	2168	12282
Fine	149865	7481	12332

The simulation setup was checked against simple geometries, for example against a cube or square of water changing phase. This can be analytically calculated and therefore was compared and showed no deviation.

4.2. Simulation results

One of the goals of the simulation was to create a fin design that could lead to a good temperature distribution over a large cross-sectional fin area and hence, over the entire storage module. Fig. 8 shows the temperature distribution in the analyzed fin. Further development in the fin design has since occurred to yet optimize this distribution. However, experimental testing of the new design has not yet been possible.

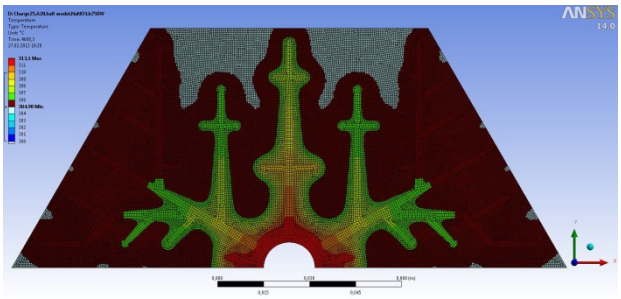

Fig. 8: Temperature distribution in phase change simulation

To compare simulation and experimental results, experimental boundary conditions were applied in the simulation. Fig. 9 shows simulation results of the half-fin model.

A first analysis of the simulation results is for plausibility based on experience from other experiments. The form of the curves and order in which the temperature probes end the phase transition is plausible. The temperature probe calculations show a steep temperature incline from 280 °C

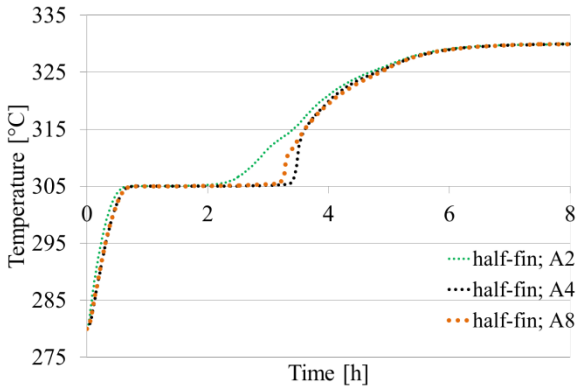

Fig. 9: Simulation results for the half-fin model

to 305 °C, then exhibit a plateau over the temperature increase to 306 °C. Above this temperature, the temperature increase is again steep until it asymptotically approached the upper temperature. The order in which the probes complete phase change (the temperature plateau) was also plausible in comparison with both the experiments and in consideration of the distance of the probes from the fin material. Temperature probe A2 (green) completed transition first and A8 (orange) last. A2 is closest to fins and A8 furthest (Fig. 3). For the half-fin simulation, the boundary conditions at the storage material sides of the model are perfectly insulated. The half-fin simulation cannot show what effect neighboring fins have on this phase change and temperature distribution. For this reason, a seven-face simulation was also completed, the results of which are compared to a half-fin simulation in Fig. 10.

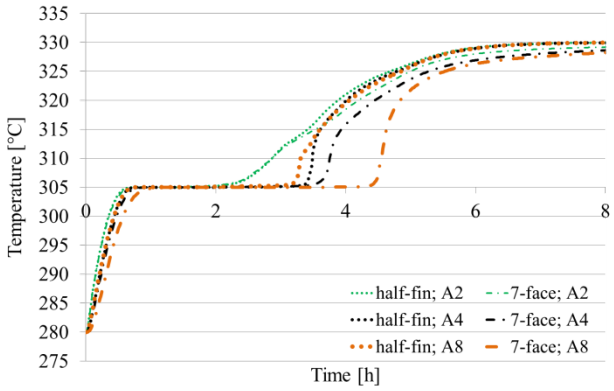

Fig. 10: Simulation results for the half-fin and seven-face model, selected temperature probes

These results show that the calculated temperatures were similar in the temperature probes closest to the central tube. Further from the tube, the results showed a larger difference, as expected. In the seven-face tube, probe A8 would be influenced by the neighboring finned tube.

5. COMPARISON OF SIMULATION AND EXPERIMENT

In order to both evaluate the model and analyze the data, experimental as well as simulated results are compared (Fig. 11). Fig. 11 shows the seven-fin simulation and experimental results of selected temperature probe calculation and thermocouple measurements. This figure shows that there are some discrepancies.

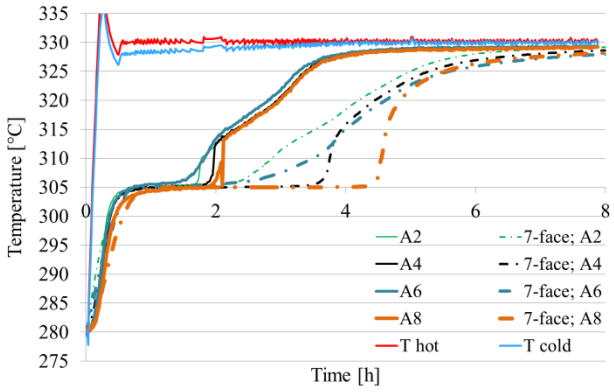

Fig. 11: Simulation and experimental results for selected temperature probes/thermocouples

It is distinctly clear that the experimental results, shown in solid lines, complete the phase change and overall charge much more quickly than the simulation calculates. Another comparison factor is the form of the curves. This is similar, though the very steep temperature change at the end of the phase change seen in the experimental results is not as pronounced in the simulated values. The temperatures of thermocouple/probe A6, shown in blue,

similarly have only a very short temperature plateau. This thermocouple is located at the tip of a finned tube.

One factor not accounted for in the simulation is the natural convection in the PCM once it has melted. Natural convection is dependent not only upon density and temperature difference but also upon the local geometry. Therefore, the value cannot be simply calculated or a factor included in the calculation that will result in an accurate result. The added component of natural convection is essentially a further reduction of the heat transfer resistance. To approximately attain this resistance reduction, one of the other resistance factors could be adapted. In order to account for this, the coefficient of thermal conductivity k in the melted PCM was adjusted to be higher. However, there is no way to calculate an adjusted conductivity value, so that this method can only be viewed as an empirical factor. The results show a better accuracy with this increased conductivity (see Fig. 12).

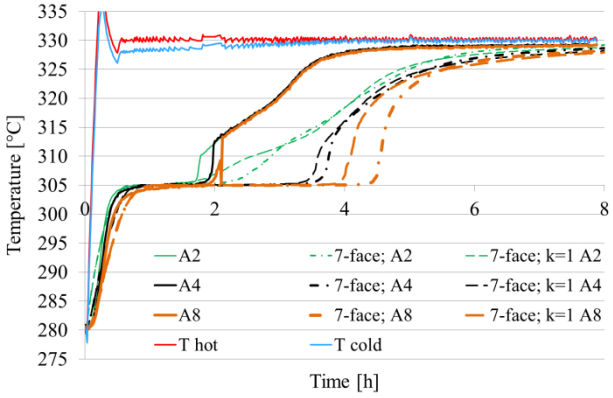

Fig. 12: Simulation results with an increased k=1 for molten salt

Natural convection is one factor that would affect calculated results. Another important factor is the rate of heat transfer from the HTM to the tube h. To evaluate this, simulations were conducted with higher heat transfer coefficients. Logically, phase change times were shortened through this factor. With an h=2000 W/m², the phase change time was approximated. However, this heat transfer coefficient was very high and as yet cannot be justified.

A further criterion is the actual heat transferred. However, due to the losses discussed above, this comparison was only practicable for larger storage units and is not presented here.

Due to the limited possibilities for obtaining experimental data with which to compare the simulation model, results from this lab unit are the only ones to date to compare with it. Other storage units have geometries requiring a three-dimensional model or other simulation set-up, so that a direct comparison has not been possible.

6. CONCLUSION AND OUTLOOK

In this paper, the results from an experimental test setup of a high temperature latent heat storage module are compared with a two-dimensional simulation of the finned-tube structures in the storage unit. The simulation model used known material properties and results in similarly formed curves. There were differences in phase change times, however. A reason for this could be due to the natural convection in the molten salt, which is not accounted for in the simulation. An approximation was simulated with an adjusted thermal conductivity coefficient for molten PCM, which showed a better phase change time while retaining the form of the curves. In future work, the natural convection in PCMs will be researched in order to better understand the effects on the rate of phase change and heat transfer.

7. REFERENCES

(1) Tamme, R., Bauer, T., Buschle, J., Laing, D., Mueller-Steinhagen, H., & Steinmann, W.-D., Latent heat storage above 120 °C for applications in the industrial process heat sector and solar power generation, Journal of energy Research, 032736017(July 2007), 264-271, doi:10.1002/er, 2008

(2) Laing, D., Bahl, C., Eickhoff, M., Fiss, M., Hempel, M., Meyer-Grünefeldt, M., Test Results of a Combined Storage System for Parabolic Trough Power Plants with Direct Steam Generation, Proceedings of ASME 5th International Conference on Energy Sustainability, 2011

(3) Laing, D., Bauer, T., Breidenbach, N., Hachmann, B., Johnson, M., Development of high temperature phase-change-material storages, Journal of Applied Energy, http://dx.doi.org/10.1016/j.apenergy.2012.11.063, 2013

(4) Mehling, H., Cabeza, L. F., Heat and cold storage with PCM, Berlin, Springer Verlag, 2008

(5) Bauer, T., Hachmann, B., Heat transfer tube, International Patent, WO 2011/069693 A1, filed July 6, 2010 and issued June 16, 2011

(6) Bauer, T., Approximate analytical solutions for the solidification of PCMs in fin geometries using effective thermophysical properties, International Journal of Heat and Mass Transfer, 54(23-24), 4923-4930. Elsevier Ltd., doi:10.1016/j.ijheatmasstransfer.2011.07.004, 2011

(7) Bauer, T., Laing, D., Kröner, U., Tamme, R, Sodium nitrate for high temperature latent heat storage, 11th International Conference on Thermal Energy Storage (Effstock), Stockholm, Sweden, 2009